Published in final edited form as:
Radiat Prot Dosimetry. 2010 March ; 138(4): . doi:10.1093/rpd/ncp278.

DOSE REDUCTION IN CT USING BISMUTH SHIELDING: MEASUREMENTS AND MONTE CARLO SIMULATIONS

Kyung-Hwan Chang,
Department of Radiologic Science, Korea University

Wonho Lee,
Department of Radiologic Science, Korea University

Dong-Myung Choo,
Department of Radiologic Science, Korea University

Choon-Sik Lee, and
Department of Nuclear and Radiological Engineering, University of Florida

Youhyun Kim
Department of Radiologic Science, Korea University

Abstract

Objective—In this research, using direct measurements and Monte Carlo calculations, we evaluated the potential dose reduction achieved by bismuth shielding in computed tomography. Patient dose was measured using an ionization chamber in a polymethylmethacrylate (PMMA) phantom which had five measurement points at the center and periphery. We performed simulations using the MCNPX code. For both the bare and the bismuth-shielded phantom, the differences of dose values between experiment and simulation were within 9%. The dose reductions due to the bismuth shielding were 1.2–55% depending on the measurement points, X-ray tube voltage, and the type of shielding. The amount of dose reduction was significant for the position covered by bismuth shielding (34–46% for head and 41–55% for body phantom in average) and negligible for other peripheral positions. The artifact on the reconstructed images were minimal when the distance between the shielding and the organs was more than 1 cm, and hence the shielding should be selectively located to protect critical organs such as the eye lens, thyroid, and breast. The simulation results using PMMA phantom was compared with those using a realistically voxelized phantom (KTMAN-2). For eye and breast, the simulation results using PMMA and KTMAN-2 phantom were similar with each other while, for thyroid, the simulation results were different due to the discrepancy of locations and the size of phantoms. The dose reductions achieved by bismuth and lead shielding were compared with each other and the results showed that the difference of the dose reductions achieved by two materials was less than 2~3 %.

INTRODUCTION

Since the development of the computed tomography (CT) in 1972, the usage of routine CT examinations has increased rapidly. Simultaneously, concerns about radiation protection and patient dose have increased in clinic because of the greater availability of multi-detector computed tomography (MDCT) which provides faster images for larger volumes but gives large doses to patients. In recent years, MDCT has been reported as an essential diagnostic imaging tool and a main part of diagnostic radiologic examinations. According to the

Corresponding author: Wonho Lee, Department of Radiological Science, Korea University College of Health Science, Seoul 136-703, Korea, wonhol@korea.ac.kr.

International Commission on Radiological Protection (ICRP 102), CT studies have increased more than 800% globally in past decades [(1)]. The increased use of multi-detector computed tomography results in greater individual patient doses and collectively greater doses to the patient population. Therefore, it is prudent and reasonable to explore methods for reducing patient doses in MDCT examinations.

The important protection concept when dealing with patient doses from MDCT is “keep as low as reasonably achievable” (the ALARA principle). Physicians, radiologists, physicists, and radiologic technologists must recognize the risk of the patient dose during CT examinations and suggest various and appropriate protocols in order to reduce the dose to radiosensitive organs such as the eye lens, thyroid gland, and reproductive organs.

Several investigators have studied methods for reducing patient doses CT examinations [(2–13)]. For example, Kostas Perisinakis showed that the dose reduction caused by a 20° angled scanning of the brain was approximately 33% [(2)]. Kenneth D. Hooper *et al.* demonstrated that eye shielding decreased radiation dose 48.5–65.4 %. C. Hohl and J. E. Wildberger showed that shielding reduced dose 47% for the thyroid and 32% for the breast during MDCT [(9)]. J. Geleijns *et al.* evaluated the dose reduction that results from in-plane shielding. According to their research, the dose reduction from lens shielding is 27% and from thyroid shielding is 26% [(10)]. J.E. Ngaile *et al*. demonstrated that lead shields of 0.25 mm thickness affect the protection of the superficial organs for head CT examination. The entrance surface doses (ESDs) of the eye lens and thyroid reduced 44 and 51%, respectively [(11)]. U. Lechel proved that an automatic exposure control systems decreased the dose by between 27% and 40% [(14)]. However, we were unaware of studies comparing potential reductions in patient dose to the most critical organs and tissues for a multitude of shielding types.

The purpose of the present study is to evaluate the CT dose reduction at five specific points of a head and body phantom with the eye, thyroid, and breast shielding, using the Monte Carlo method and experimental measurements with the polymethylmethacrylate phantom (PMMA phantom, 76-419-4150, Fluke biomedical, Cleveland, OH, USA).

MATERIALS AND METHODS

Monte Carlo simulation

We used the Monte Carlo N-Particle Transport Code (MCNPX code, Los Alamos National Laboratory, the University of California, CA, USA) to simulate the CT dose for a PMMA phantom. The focal size of the X-ray was $7.579 \times 7.579\ mm^2$, and the focal spot was located 541 mm from the center of the CT system. The angular width and thickness of the fan beam was 49° and 54mm, respectively.

Figure 1 shows a 120-keV X-ray spectrum analyzed using the SRS-78 program (Birch and Marshall, Institute of Physics and Engineering in Medicine, 1997) to simulate the beam quality of the CT system. A bowtie filter was estimated from the calculation based on the dose difference per unit distance from the center of the CT system. As shown in Equation 1, the normalization factor (NF), which was used to convert simulation results into experimental data, was defined by the ratio of the dose (K_{sim}) evaluated by simulation to the measured dose (K_{mea}) under the same conditions. In both the simulation and the experiment used to obtain NF, an ionization chamber was positioned in the center of the CT system without any phantom or shielding. Since the conditions of simulation and measurement were identical to each other, the NF value was independent of positions in the field of view (FOV).

The absorbed dose in the phantom was calculated by the NF and other factors as shown in Equation 2:

$$\mathrm{NF\,(mGY/Photon)}=\mathrm{K_{sim}/K_{air}} \quad (1)$$

$$\mathrm{D_{air}}=\mathrm{D_{sim}}\times \mathrm{NF}\times \mathrm{mAs/rotation}\times \mathrm{N} \quad (2)$$

where D_{sim} is the dose evaluated by the simulation and N is the number of rotations.

Figure 2 shows the simulations of the phantom, ionization chamber, and bismuth shielding used to calculate the absorbed dose in the phantom. Figure 2(a) is an axial view showing the ionization chamber, exterior cap, and PMMA phantom without bismuth shielding. Figures 2(b) and 2(c) are the frontal views of phantom with bismuth shielding and its magnified picture, respectively. Using MCNPX code, the simulation result with the PMMA phantoms was compared with that with a realistically voxelized phantom, KTMAN-2 (cf. Figure 3) made by C. Lee[15].

We also compared the effect of the dose reduction between the lead and bismuth. The MCNPX simulation for the lead carried out on the same experimental condition for the bismuth.

Experimental conditions

The CT dose was measured by a CT ionization chamber (Model 20 × 5-3 CT, S/N 21560; Radcal corporation, Monrovia, USA) in a polymethylmethacrylate phantom (PMMA phantom, head and body phantom, 76-419-4150, Fluke Biomedical) which had five measurement points at the center and periphery. The chamber consists of C552, electrode, and polyacetal exterior cap. C552 was air-equivalent wall composed of hydrogen, carbon, oxygen, fluorine and silicon. The length and active volume of the chamber were 10cm and 3 cm^3. The density of the exterior cap and C552 were 1.41 g/cm^3 and 1.76 g/cm^3. The PMMA head and body phantoms are made of solid acrylic and five cylindrical holes located at the center and at directions of 12, 3, 6, and 9 o'clock from the center. The diameters of the head and body phantom were 16 cm and 32 cm, respectively. The diameter of the holes was 1.31cm, and each hole was 1 cm from the edge of phantom. This location was close to eyes, thyroid and the inside of breast. Bismuth shielding for eyes, thyroid and breast was made by F&L Medical Products (Vandergrift, PA, USA). The sizes of eye, thyroid and breast shielding were 14×3.5×0.32 cm, 15×8.5×0.48 cm and 53×20.5×0.43 cm, respectively. The density of the bismuth shielding was approximately 0.7 g/cm^3. Every shielding was attached around phantoms as shown in Figure 6.

The sensitive volume of the ionization chamber was aligned with the center of the CT system. Dose was measured five times at each hole to calculate an average value. The dose with and without bismuth shielding around the PMMA phantom was compared to calculate dose reduction. For the dose measurements of the head, CT scanning was performed with eye and thyroid shielding on the PMMA head phantom. For the dose measurements of the body, the PMMA body phantom was used with breast shielding. The X-ray high voltages were 120 kVp and 80 kVp, which are standard values in X-ray diagnosis. The current and exposure time were 100mA and 0.1sec, which are common conditions in CT examination.

RESULTS

As shown the Tables 1–3, for both bared and shielded PMMA phantoms, the differences in dose between the experiment and simulation were 9% or less. For eye dose, the averaged

doses measured and simulated without the shielding were 3.26 and 3.43 mGy, and those with the shielding were 2.87 and 3.02 mGy at 120 kVp. At 80 kVp, the averaged dose measured and simulated without the shielding were 1.15 and 1.21 mGy, and those with shielding were 0.98 and 1.02 mGy. For thyroid dose, the values of the averaged dose measured and simulated without the shielding were 3.26 and 3.43 mGy, and those with shielding were 2.82 and 3.00 mGy at 120 kVp. The measured and simulated doses were reduced from 1.15 and 1.21 mGy to 0.95 and 1.01 mGy at 80 kVp. For breast study, the averaged doses measured and simulated with shielding were 1.55 and 1.53 mGy and those without shielding were 1.34 and 1.34 mGy at 120 kVp. The averaged doses measured and simulated at 80 kVp were reduced from 0.53 and 0.50 mGy to 0.44 and 0.43 mGy.

For the bare phantom, the dose was highest at the 12 o'clock and lowest at the 6 o'clock position in all cases. This positional dependency of dose was due to the radiation attenuation in the couch. The dose deposited in the body phantom was much lower than that deposited in the head phantom since the dose attenuation in the phantom was proportional to the size of the phantom. Figure 5 shows that bismuth shielding reduced the dose by 1.2 to 55% depending on the measurement position, X-ray tube voltage, and type of shielding.

The dose reductions were highest for the 12 o'clock position since it was closest to the bismuth shielding. The average dose reduction value was an about 34–46% and 41–55% at the 12 o'clock positions of the head and body phantom depending on the tube voltages and types of shielding.

The dose reductions at the center were approximately one-third of those at 12 o'clock, and there were only slight reductions at the other peripheral positions. We concluded that the differences between dose reductions at each evaluation point were related to the distance from the area covered by bismuth shielding. For 12 o'clock and the center position, the dose reduction was inversely proportional to the X-ray high voltage since the stopping power of bismuth shielding decreases with X-ray energy.

Due to the radiation attenuation in the bismuth shielding, the reconstructed CT image can be distorted. As shown in the Figure 6, the image distortion due to the bismuth shielding was limited in the range of 1 cm from the shielding, and hence it is encouraged to make more than 1 cm distance between the shielding and critical organs to be diagnosed.

The amount of doses for PMMA and KTMAN-2 was compared with each other in Table 4. The doses for the PMMA phantom measured by the ionization chamber and those for the breast of KTMAN-2 phantom were multiplied by the ratio of the total cross-sectional area to the X-ray exposed area of the ionization chamber or the breast because all area of the eye and thyroid were exposed by X-ray while only partial area of the ionization chamber and breast was in the angular range of incident X-ray. The difference of doses for PMMA and KTMAN-2 was approximately 1% for eye, 38% for thyroid and 9% for breast. For the eye, the location of the organ was close to that of the hole located in the 12 o'clock position of PMMA head phantom and the whole size of the head in KTMAN-2 was also close to that in PMMA phantom. In result, the difference of doses between the 12 o'clock position of PMMA head phantom and the eye of KTMAN-2 was negligible. However, the thyroid of KTMAN-2 was located near center and the size of the neck in KTMAN-2 was much smaller than that of PMMA head phantom, and hence the difference of thyroid doses between two phantoms was not small. In the case of breast, the thickness of body in KTMAN-2 and that in PMMA phantom were close to each other but the location of the breast in KTMAN-2 and that of the hole in PMMA phantom was not exactly same resulting in difference in the estimated dose.

As shown in Table 5, the dose reduction by bismuth shielding was compared with that by lead shielding with same size, density and thickness. The reduced doses were calculated by MCNPX code for five points of PMMA phantom and averaged. The simulation results showed that the difference in the dose reductions of two materials was less than 2~3%.

DISCUSSION

Since introduction of CT in the 1970s, the use of CT has significantly increased. With the development of MDCT, the importance of patient protection has been raised. Thus, in this paper, we evaluated and verified the effect of bismuth shielding for various specific points in head and body phantoms during CT examination. The amount of dose reduction was strongly dependent on the positions. In particular, the dose reduction was highest at the12 o'clock position, while there were almost no dose reductions at the 3, 6, and 9 o'clock positions. Therefore, it is important to apply bismuth shielding for most CT examinations to selectively protect critical organs such as eyes, thyroid, and breast located near the surface, which decreases the probability of side effects such as cataracts and thyroid and breast cancer after multiple CT exams. Bismuth shielding should be selectively located to avoid the significant degradation of the image quality. If the shielding is more than 1 cm apart from the organ to be diagnosed, the artifact caused by the shielding is minimized. In addition, before applying the shielding to patients, it is necessary to consult with radiologists in order to guarantee that the artifacts caused by the shielding are acceptable in the medical diagnosis.

Both exposure dose and dose reduction were dependent on the X-ray tube voltage because the X-ray energy was inversely proportional to the attenuation in phantom and bismuth shielding. However, there was no perfect recommendation for proper voltage for optimizing image quality and dose reduction because the each clinic has its own protocols, scan controlling techniques and equipments for each patient.

The simulation result was well matched with experimental data, and hence we concluded that it was reasonable to use simulation for the dose estimation of complex designs which were difficult to be tested by experiments. The simulation results of PMMA and KTMAN-2 phantom were almost same for eye and breast, but different for thyroid due to the discrepancy of the locations of the organs and the sizes of the phantoms. Therefore, the simulation result using PMMA phantom was applicable to an actual patient for eye and breast but not for thyroid. In general, doses of some organs near surface such as eye and breast could be calculated using PMMA phantom and other organs whose location and size was different from those of PMMA phantom could be estimated using realistically voxelized phantom such as KTMAN-2.

We compared the dose reductions achieved by the bismuth and lead which were well known materials for radiation protection. The difference of the dose reduction was about 2~3 % in all cases. This difference is very much like that of the result of other investigator [(3)].

There were limitations in our research. First, the effect of the bismuth shielding could be further studied in the viewpoint of image quality. The dose reduction using the bismuth shielding was proven to be significant and the image distortion due to the shielding was minimal if the distance between phantom and shielding was more than 1 cm, but the condition may be changed depending on the experimental conditions such as space modulated X-ray exposure in automated CT system to improve the reconstructed image quality with shielding. We plan to study in detail about the relationship between the image quality and the thickness of the bismuth shielding with automated exposure system.

Second, we focused on the adult model during this study. However, since the radio sensitivity of pediatric patients is higher than that of adults, the effect of dose reduction with bismuth is also important for children. In the future, therefore, we will study the effect of dose reduction with bismuth shielding for pediatric patients.

CONCLUSION

In this paper we have reported the effective performance of shielding used to reduce the unnecessary radiation dose of CT examinations. 1) With proper distance between critical organs and shielding, the dose of the critical organs could be significantly reduced without degrading the image quality. 2) Bismuth and lead showed similar performance as shielding materials. 3) For eye and breast, the simulation results using PMMA phantom were similar with those using realistically voxelized phantom, which was not applicable for thyroid whose location and the amount of surrounding material were different for each phantom.

Acknowledgments

The authors would like to thank the head and members of the radiology department, Kyung Hee Medical Center, for providing its MDCT facility. This work was supported by a 3N Researcher Program through the National Research Foundation of Korea (NRF) funded by the Ministry of Education, Science and Technology.

References

1. International Commission on Radiological Protection. Annals of the ICRP. 2007. Managing Patient Dose in Multi-detector Computed Tomography (MDCT). ICRP publication 102.
2. Perisinakis K, Raissaki M, Tzedakis A, Theocharopoulos N, Damilakis J, Gourtsoyiannis N. Reduction of eye lens radiation dose by orbital bismuth shielding in pediatric patients undergoing CT of the head: A Monte Carlo study. Med Phys. 2007; 32:1024–1030. [PubMed: 15895586]
3. Hopper KD, Neuman JD, King SH, Kunselman AR. Radioprotection to the Eye During CT scanning. AJNR Am J Neuroradial. 2001; 22:1194–1198.
4. McLaughlin DJ, Mooney RB. Dose reduction to radiosensitive tissues in CT. Do commercially available shields meet the user's needs? Clinical Radiology. 2003; 59:446–450. [PubMed: 15081850]
5. McCollough CH, Bruesewitz MR, Kofler JM. CT dose reduction and dose management tools: Overview of available options. RadioGraphics. 2006; 26:503–512. [PubMed: 16549613]
6. Fricke BL, Donnelly LF, Frush DP, Yoshizumi T, Varchena V, Poe SA, Lucaya J. In-plane bismuth breast shields for pediatric CT: effects on radiation dose and image quality using experimental and clinical data. AJR. 2003; 180:407–411. [PubMed: 12540443]
7. Coursey C, Frush DP, Yoshizumi T, Toncheva G, Nguyen G, Greenberg SB. Pediatric Chest MDCT Using Tube Current Modulation: Effect on Radiation Dose With Breast Shielding. AJR. 2008; 190:W54–W61. [PubMed: 18094273]
8. Kalra MK, Dang P, Singh S, Shepard JO. In-plane shielding for CT: effect of off-centering, automatic exposure control and shield-to-surface distance. Korean J Radiol. 2009; 10:156–163. [PubMed: 19270862]
9. Hohl C, Wildberger JE, Sub C, Thomas C, Muhlenbruch G, Schmidt T, Honnef D, Gunther RW, Mahnken AH. Radiation dose reduction to breast and thyroid during MDCT: Effectiveness of an in-plane bismuth shield. Acta Radiologica. 2006; 47(6):562–567. [PubMed: 16875333]
10. Geleijns J, Artells MS, Veldkamp WJH, Tortosa ML, Cantera AC. Quantitative assessment of selective in-plane shielding of tissues in computed tomography through evaluation of absorbed dose and image quality. Eur Radiol. 2006; 16:2334–2340. [PubMed: 16604323]
11. Ngaile JE, Uiso CBS, Msaki P, Kazema R. Use of lead shields for radiation protection of superficial organs in patients undergoing head CT examinations. Radiation Protection Dosimetry. 2008; 130(4):490–498. [PubMed: 18375945]

12. Yilmaz MH, Albayram S, Yasar D, Ozer H, Adaletli I, Selcuk D, Akman C. Female breast radiation exposure during thorax multidetctor computed tomography and the effectiveness of bismuth breast shield to reduce breast radiation dose. J Comput Assist Tomogr. 2007; 31:138–142. [PubMed: 17259846]

13. Honnef D, Mahnken AH, Haras G, Wildberger JE, Staatz G, Das M, Barker M, Stanzel S, Gunther RW, Hohl C. Pediatric Multidetector Computed Tomography Using Tube Current Modulation and a Patient Image Gallery. Acta Radiologica. 2008; 49(4):475–483. [PubMed: 18415795]

14. Lechel U, Becker C, Langenfeld-Jager G, Brix G. Dose reduction by automatic exposure control in multidetector computed tomography: comparison between measurement and calculation. Eur Radiol. 2008; 19:1027–1034. [PubMed: 18987864]

15. Lee, C. KTMAN-2 (Korean Typical MAN-2). Korean voxel phantom. http://mcnp-green.lanl.gov/publication/mcnp_publications.html#medicalphysics

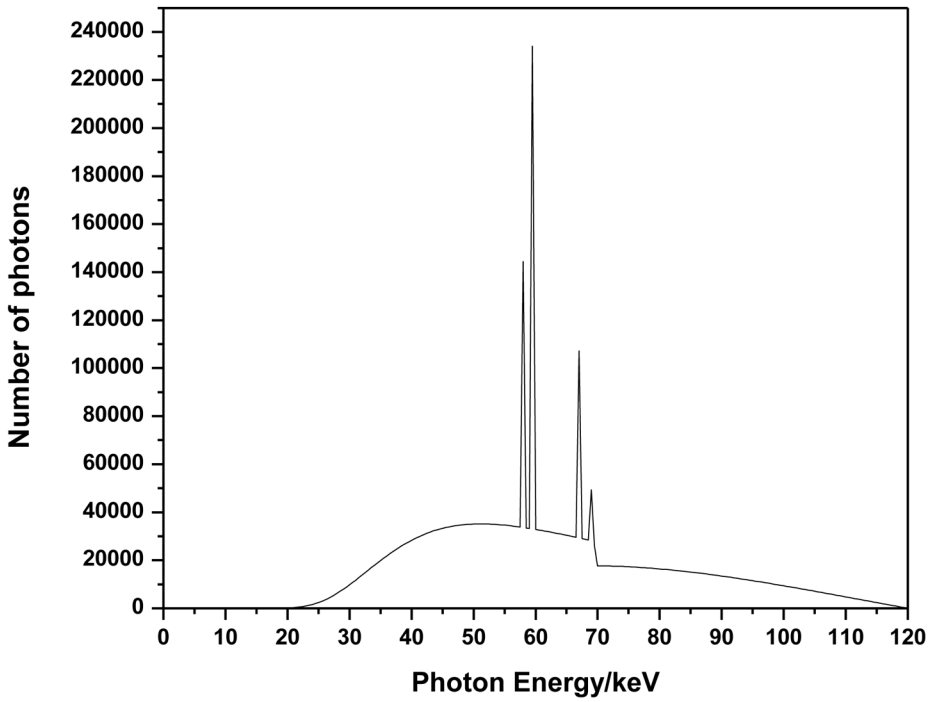

Figure 1.
X-ray spectrum from tungsten target and aluminum filter at 120 kVp

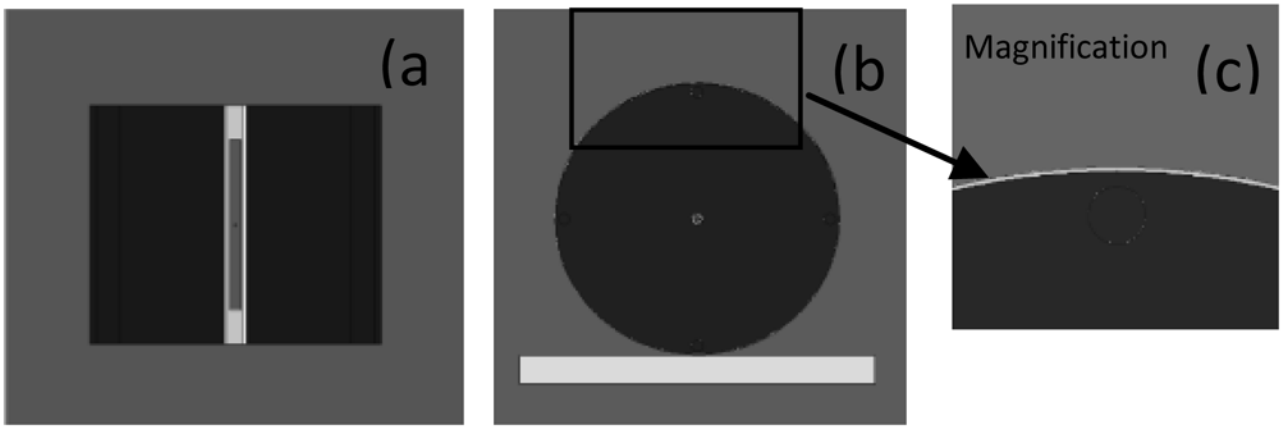

Figure 2.
Phantom, bismuth shielding and ionization chamber simulated by MCNPX code.
(a) Axial view, (b) Frontal view, (c) Magnified picture of bismuth shielding on the phantom

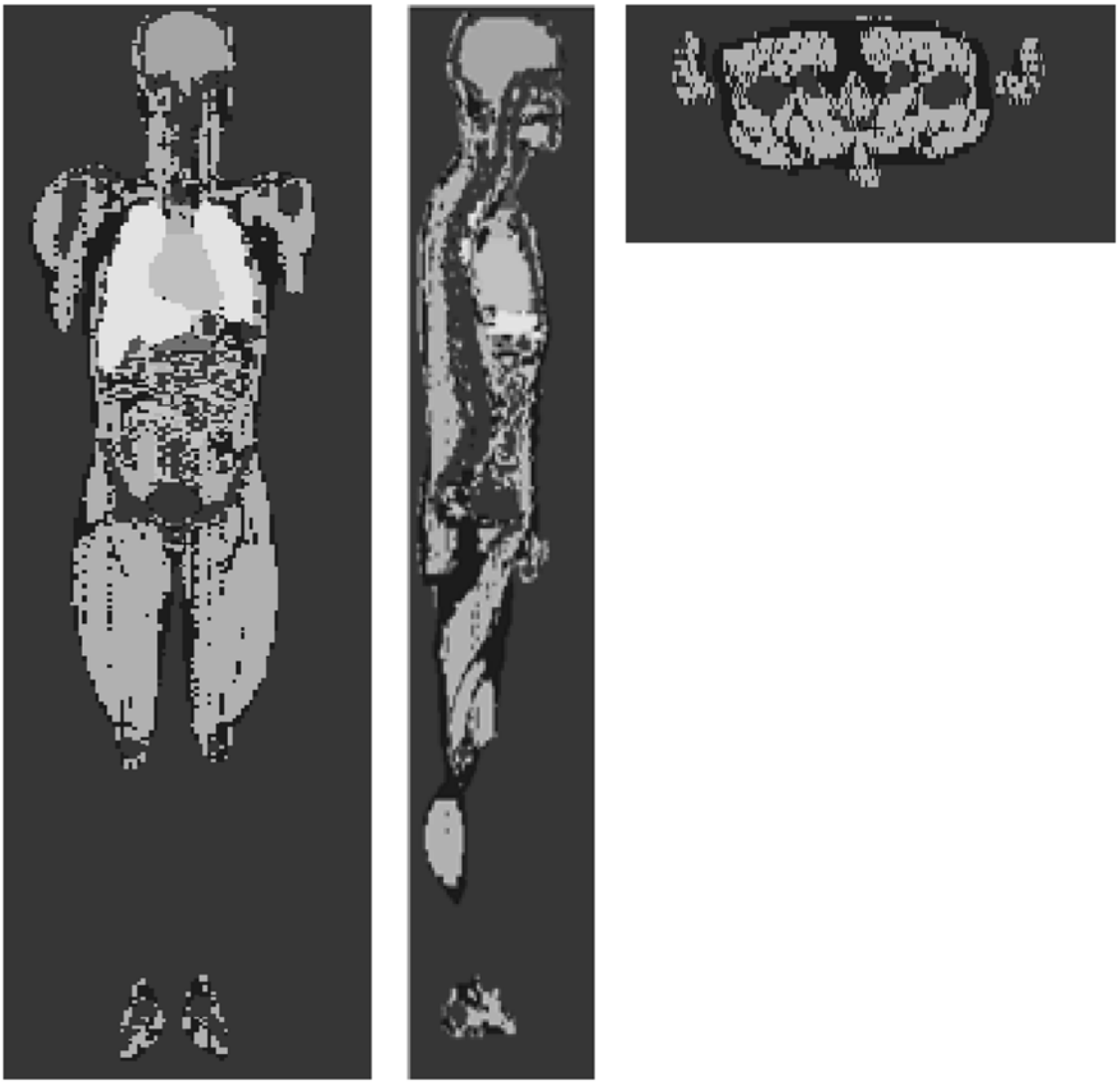

Figure 3.
Korean Typical MAN-2 (KTMAN-2) phantom simulated by MCNPX code. (a) Coronal view, (b) Sagittal view, (c) Axial view

Figure 4.
Ionization chamber, PMMA phantom and bismuth shielding for CT dose measurement.

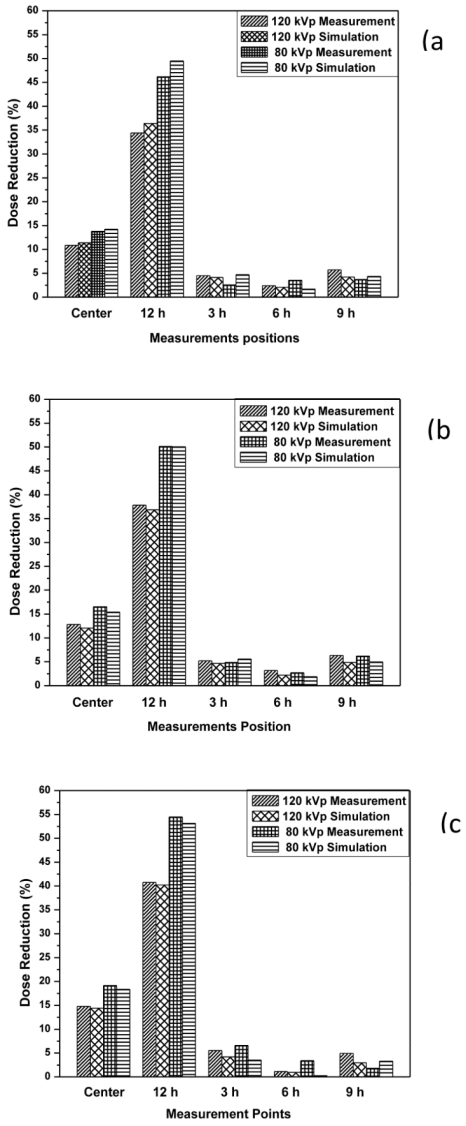

Figure 5.
Dose reductions achieved using bismuth shielding for (a) eyes (b) thyroid and (c) breast.

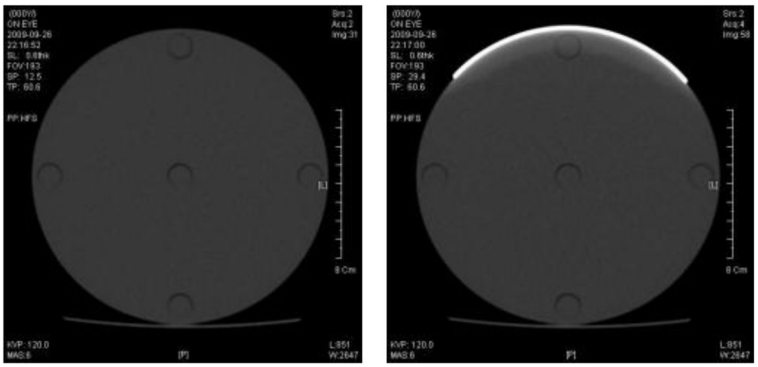

Figure 6.
CT scan images of the PMMA head phantom for 120 kVp and 6mAs.
(a) without shielding (b) with eye shielding.

Table 1

The differences in dose values between experiment and simulation with and without eye bismuth on the head phantom(mGy).

Position	kVp	Head phantom without bismuth			Head phantom with bismuth		
		Mea	Sim	Differ(%)	Mea	Sim	Differ(%)
Center	120	3.24	3.41	−5.52	2.88	3.03	−4.90
	80	1.08	1.13	−5.01	0.93	0.97	−4.47
12h	120	3.45	3.59	−4.06	2.27	2.29	−0.92
	80	1.26	1.29	−2.43	0.68	0.65	3.85
3h	120	3.24	3.43	−5.83	3.10	3.29	−6.23
	80	1.14	1.24	−8.79	1.11	1.18	−6.41
6h	120	3.04	3.27	−7.56	2.97	3.20	−7.91
	80	1.07	1.14	−6.05	1.04	1.12	−8.09
9h	120	3.30	3.44	−4.09	3.12	3.30	−5.77
	80	1.17	1.24	−5.52	1.13	1.18	−4.81

[1]Mea: Measurement, Sim: Monte Carlo simulation, Differ: Difference between measurement and simulation.

Table 2

The differences in dose values between experiment and simulation with and without thyroid bismuth on the head phantom (mGy).

Position	kVp	Head phantom without bismuth			Head phantom with bismuth		
		Mea	Sim	Differ(%)	Mea	Sim	Differ(%)
Center	120	3.24	3.41	−5.52	2.82	3.00	−6.44
	80	1.08	1.13	−5.01	0.90	0.96	−6.40
12h	120	3.45	3.59	−4.06	2.15	2.27	−5.64
	80	1.26	1.29	−2.43	0.63	0.64	−2.57
3h	120	3.24	3.43	−5.83	3.07	3.27	−6.45
	80	1.14	1.24	−8.79	1.09	1.17	−7.95
6h	120	3.04	3.27	−7.56	2.95	3.20	−8.62
	80	1.07	1.14	−6.05	1.05	1.12	−7.01
9h	120	3.30	3.44	−4.09	3.10	3.28	−5.75
	80	1.17	1.24	−5.52	1.10	1.18	−6.93

[1]Mea: Measurement, Sim: Monte Carlo simulation, Differ: Difference between measurement and simulation

Table 3

The differences in dose values between experiment and simulation with and without breast bismuth on the body phantom (mGy).

Position	kVp	Body phantom without bismuth			Body phantom with bismuth		
		Mea	Sim	Differ(%)	Mea	Sim	Differ(%)
Center	120	0.95	0.97	−2.28	0.81	0.83	−2.75
	80	0.27	0.26	5.14	0.22	0.21	4.22
12h	120	1.75	1.70	2.68	1.03	1.01	1.81
	80	0.62	0.58	6.45	0.28	0.27	3.74
3h	120	1.75	1.71	2.67	1.66	1.64	1.33
	80	0.62	0.58	6.12	0.58	0.56	2.99
6h	120	1.51	1.54	−1.95	1.50	1.53	−2.14
	80	0.51	0.52	−0.16	0.50	0.51	−3.40
9h	120	1.77	1.73	2.39	1.68	1.68	0.36
	80	0.63	0.59	7.52	0.62	0.57	8.94

[1]Mea: Measurement, Sim: Monte Carlo simulation, Differ: Difference between measurement and simulation

Table 4

The differences in dose using PMMA and realistic voxel phantom (mGy).

120kVp	**PMMA (12h)**	**KTMAN-2**	**Difference (%)**
Head	5.99	6.03	0.67
thyroid	5.99	9.62	−37.73
Breast	3.15	3.49	−8.31
80kVp	PMMA (12h)	KTMAN-2	Difference (%)
Head	2.15	2.12	1.42
thyroid	2.15	3.44	−37.50
Breast	0.48	0.44	9.09

Table 5

The differences in dose reductions using bismuth and lead for head and body phantoms.

120kVp	Shielding material	Averaged dose with shielding	Dose reduction (%)
Head	Bismuth	3.02	11.95
	Lead	2.95	13.99
thyroid	Bismuth	3.00	12.54
	Lead	2.94	14.29
Breast	Bismuth	1.34	12.42
	Lead	1.31	14.38
80kVp	Shielding material	Averaged dose with shielding	Dose reduction (%)
Head	Bismuth	1.02	15.70
	Lead	0.99	18.18
thyroid	Bismuth	1.01	16.53
	Lead	0.98	19.01
Breast	Bismuth	0.43	14.00
	Lead	0.41	18.00